NEAR-INFRARED IDENTIFICATION AND SORTING OF POLYLACTIC ACID

Namrata Mhaddolkar *, Gerald Koinig and Daniel Vollprecht

Waste Processing Technology and Waste Management (AVAW), Montanuniversität Leoben, Franz-Josef-Straße 18, 8700 Leoben, Austria

ABSTRACT

Biobased plastics are often seen to be an environmentally friendly alternative to conventional plastics, with their share, though being less now, is gradually increasing. This necessitates that the waste management of these possibly eco-friendly materials is also at par with their growth. Near-infrared (NIR) sorting is an effective waste sorting technology and is already widely used for conventional plastics. Thus, it would be imperative to analyse whether this effective existing infrastructure could also be successfully used to sort bioplastic. In the present study, the lab-scale NIR sensor-based sorting system in Montanuniversität Leoben was used to analyse polylactic acid (PLA) in three sets of experiments. First, the spectra of 7 conventional plastics were compared to that of virgin PLA and it was found that PLA has a distinct spectrum and should ideally be detected from a mixed plastic fraction. Second, it was assessed whether different grades and thicknesses of virgin PLA samples produced different spectra and it was found that there is a slight difference in the intensities without any wavelength shift of the recognizable peaks. Lastly, the detection of 10 PLA product samples was tested using the NIR recipe of a virgin PLA. It was observed that the samples were successfully detected and blown out as PLA for all the conducted trials. Additionally, it was also seen that an appropriate backlight setting is important to be able to correctly sort the transparent PLA products in the used chute-type sorter.

1. INTRODUCTION

Biobased plastics are often seen as an environmentally friendly alternative to conventional plastics with an important role in fighting the problem arising from plastic pollution of the environment (Calabrò & Grosso, 2018). Biobased non-biodegradable plastics (e.g. biodegradable polyethylene terephthalate (bio-PET)), also known as drop-in plastics, could be recycled in conventional plastic recycling plants. However, bio-based biodegradable plastics (hereafter referred to as bioplastics) have a different fate. They are mostly incinerated, as due to their still very small share in lightweight packaging waste no recycling route has been established yet. Although incineration of bioplastics is characterized by carbon neutrality (Lorber et al., 2015), the waste hierarchy prefers recycling (EU Waste Framework Directive, 2008). As the market share of bioplastics today is expected to grow dynamically in the coming years (Briassoulis et al., 2020), the investigation of recycling options for bioplastics is highly promising.

With a vast existing infrastructure available for plastic waste management, it is imperative to analyse whether the same could be used for bioplastics and what level of changes would be required to allow the recycling of bioplastics. Within this study, the suitability of the existing sorting infrastructure for the processing of bioplastic waste was assessed. For this purpose, NIR sorting technology, which is a widely used plastic sorting technology material (Bonifazi et al., 2021; Helena Wedin et al., 2017; G. Koinig et al., 2022; Gerald Koinig et al., 2022; Zhu et al., 2019), was used to check the sortability of bioplastics.

NIR sensor-based sorting technology is based on the principle of spectroscopy, where the absorption of electromagnetic radiation in the NIR region (700 to 2500 nm), due to the vibration of the chemical bonds at a particular wavelength produces a signature spectrum for a particular material (Helena Wedin et al., 2017; Zhu et al., 2019). A NIR sorting system uses a NIR spectral database which is prepared based on appropriate waste samples. Rani et al. (2019) prepared a NIR spectral database from a large number of plastic waste samples from a waste recycling plant, which was then used for testing the sorting of 5 conventional plastic fractions with a miniature NIR spectrometer. Also, Helena Wedin et al. (2017) used four market-available NIR sorters to sort textile post-consumer waste. They used an existing NIR database as well as created a new

one for their analyses. Wu et al. (2020) conducted a test to see whether using only virgin materials to teach their sorter could sort the waste electrical and electronic equipment plastic waste, and concluded that the detection was improved when they used a dataset equipped with virgin as well as actual product spectra information. Pre-processing of the data is a crucial step in NIR spectroscopy, which is prone to light scattering (J. Huang et al., 2010; Rinnan, Nørgaard, et al., 2009; Rinnan, van Berg, & Engelsen, 2009). The main function of pre-processing step is to ensure that the resulting spectra adhere to the Beer-Lambert law mentioned in the following section; in other words, the absorbance should be directly proportional to the concentration of the absorbents, sample thickness, and molar absorptivity (Masoumi et al., 2012). NIR spectroscopy combined with optimum pre-processing techniques, spectra repeatability & classification of certain plastics were improved (Zhu et al., 2019).

With a near-infrared hyperspectral image system (NIR-HIS), the spectral data is obtained as a set of hyperspectral images (or a spectral hypercube), where each image represents a spectral band or a narrow range wavelength (Amigo et al., 2015; Manley, 2014). Chemometric techniques, which enable the extraction of multivariate information from the data (Amigo et al., 2015), along with the NIR spectroscopy are well established for plastic waste sorting (Neo et al., 2022; Rani et al., 2019; Rodarmel & Shan, 2002; Wu et al., 2020). Zheng et al. (2018) used NIR-HIS along with PCA to successfully characterize and sort acrylonitrile butadiene styrene (ABS), polystyrene (PS), polypropylene (PP), polyethylene (PE), polyethylene terephthalate (PET), and polyvinyl chloride (PVC). NIR-HIS combined with partial least squares based rigorous classification models were used to successfully sort HDPE and PP by Pieszczek and Daszykowski (2019). Serranti and Bonifazi (2018) applied short wave infrared hyperspectral imaging system (SWIR-HIS) & hierarchical partial-least squares discriminant analysis (PLS-DA) for investigating PP, low-density polyethylene (LDPE), high-density polyethylene (HDPE), PS and PVC waste. NIR-HIS spectral data of polyolefins from building & construction waste was analysed by Serranti and Bonifazi (2018) using PCA. Ghasemzadeh-Barvarz et al. (2014) successfully used multi-variate image analysis with NIR-HIS to inspect multi-layer films.

PLA, when used for bottle application is similar in density and appearance to PET; therefore, NIR analyses of the two are widely conducted in the literature. NatureWorks, a PLA manufacturing company, successfully tested the sortability of PLA (Ingeo™) from PET bottles (Niaounakis, 2019). Similar tests were conducted using NatureWorks PLA bottles by Primo waters with positive results on NIR-based sortability (Müller et al., 2014). It was also concluded by Handschick et al. (2012) that it is possible to separate PLA from PET and PP bottles using NIR sorting methodology. However, PLA presence was also seen to contaminate the recycling streams of some conventional plastic streams (Alaerts et al., 2018; Gere & Czigany, 2019; Hahladakis & Iacovidou, 2018, 2019). On the other hand, Ulrici et al. (2013) concluded that it is possible to recog-

nize PET and PLA using NIR-HIS plus PLS-DA. Chen et al. (2021) determined that PLA cups could be sorted out from a combined fraction with conventional plastics (HDPE, PP, PET, and PS). Additionally, they also analysed the effect of degradation on the sortability of PLA from this mixed fraction. Cao and Sharma (2013) confirmed that it is possible to distinguish PLA using NIR, successfully supported by applicable chemometric methods.

Thus, it can be seen that PLA trials on NIR sorters were mostly conducted with PLA bottles, cups, or fibers; but there are other kinds of products available in the market (e.g. packaging films, containers). The present paper focuses on analyzing the use of NIR sensor-based sorting equipment present in Montanuniversität Leoben (MUL) for addressing the following research questions with PLA:

- Does the PLA spectrum significantly differ from that of the seven conventional plastics considered?
- A comparison between PLA and conventional plastics, which were not considered so far, was conducted.
- How does a change in grade and thickness affect the PLA spectrum?
- A visual comparison was conducted to answer the question, as well as answering the question.
- Can PLA products be detected using a recipe made from virgin PLA?
- Here, the detection and ejection of PLA products based on the virgin PLA recipe were observed, with an addition of an interesting observation.

1.1 List of abbreviations

- ABS: Acrylonitrile butadiene styrene
- HDPE: High density polyethylene
- LDPE: Low-density polyethylene
- LLDPE: Linear low-density polyethylene
- NIR: Near infrared
- NIR-HIS: Near infrared hyperspectral image system
- PCA: Principal component analysis
- PC: Principal component
- PE: Polyethylene
- PET: Polyethylene terephthalate
- PLA: Polylactic acid
- PLS-DA: Partial-least squares discriminant analysis
- PP: Polypropylene
- PS: Polystyrene
- PVC: Polyvinyl chloride
- SWIR: Short wave infrared
- TPU: Thermoplastic polyurethane
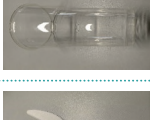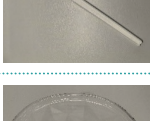- VIS: Visual spectroscopy

2. MATERIALS AND METHODOLOGY

2.1 Samples for experiments

For conducting the experiment three different types of samples were used.

2.1.1 Conventional plastic samples

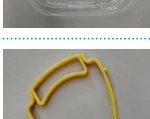Seven conventional plastic materials (Figure 1 Part A) – high-density polyethylene (HDPE), polyethylene tere-

TABLE 1: PLA product sample information.

| Sr. No.	Picture of Sample	Sample Name	Source	Quantity	Colour
1		Lid-Cup 1	Compostable packaging manufacturer	1	Matt white
2		Cup 1	Compostable packaging manufacturer	1	Transparent
3		Cup 2	Compostable packaging manufacturer	1	Transparent
4		Cutlery 1_Knife	Compostable packaging manufacturer	1	Matt white
5		Container 2	Compostable packaging manufacturer	1	Transparent
6		Cutlery 2_Spoon	Compostable packaging manufacturer	1	Matt white
7		Lid-Container-Takeaway	Restaurant	1	Transparent
8		Yellow Face Shield	3-D print lab	1	Yellow
9		White Design	3-D print lab	1	White
10		Green Bottle Opener	Private collection	1	Green
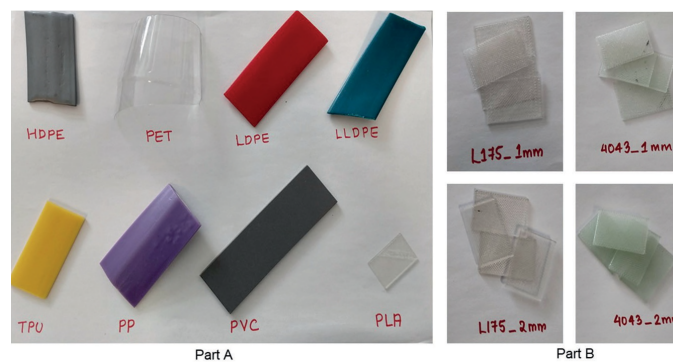
FIGURE 1: Samples for experiments, Part A – virgin conventional plastics and PLA, Part B – virgin PLA material.

phthalate (PET), low-density polyethylene (LDPE), linear low-density polyethylene (LLDPE), thermoplastic polyurethane (TPU), polypropylene (PP), and polyvinyl chloride (PVC); were obtained from Polymer Science Department (Montanuniversität Leoben, Austria).

2.1.2 PLA samples for creating a recipe

Virgin PLA samples of two different grades and thicknesses (1 mm and 2 mm each) were used for this experiment. These samples (size 20 mm x 30 mm) were 3D printed by Polymer Science Department (Montanuniversität Leoben, Austria) using the virgin PLA material procured from NatureWorks and Total Corbion. Below are details about the two different grades (Figure 1 Part B):

- PLA 4043 - Ingeo™ Biopolymer 4043D, manufactured by NatureWorks.
- PLA L175 - Luminy® L175, manufactured by Total Corbion.

2.1.3 Samples for testing recipe

A total of 10 samples were used for testing the recipe and were obtained from four different sources. Out of the 10 total samples, 6 were ordered from a compostable packaging manufacturer, 2 were failed prints from the 3-D print lab FabLab (Leoben, Austria), 1 takeaway container from a restaurant, and 1 from a private collection. Table 1 shows the list of the samples with all the important information. The six samples from the packaging manufacturer were made of two different materials (biofutura, 2021); CPLA (Lid Cup 1, Cutlery 1_Knife, Cutlery 2_Spoon) which consisted of chalk mixed with PLA giving it a matt-white colour, and pure PLA (Cup 1, Cup 2, Container 2).

2.2 Equipment used

Experiments were conducted for PLA bioplastic using a lab-scale sensor-based sorting equipment (Binder+Co AG equipped with EVK Helios NIR G2-320, Hyperspectral Imaging System 930 – 1700 nm wavelength range - Friedrich et al., 2022). The hyperspectral imaging camera has a spatial resolution of 312 effective pixels and a frame acquisition speed of 500 Hz at 216 spectral pixels. The system has a Halogen lamp HeLn Dr. Fischer 15026Z with a reflector (800 W) as the NIR light emitter. Based on the technical details of the lamp, the beam angle was "focus point" and the working distance of the hyperspectral camera is approximately 85 cm (measured manually on the instrument, as no technical details are available). The mean spectra and their variation for the mentioned samples were calculated using the clustering (Class32) method in EVK Helios Optimizer Sqalar software (Version 4.6.2019.2). The sensor-based sorting machine with the chute-type NIR setup used is shown in Figure 2 below. The sample material reflects the emitted NIR light which is captured by the hyperspectral imaging camera. Based on the data from this camera and the chosen settings, the control unit decides whether the material is to be sorted or not. Once the "to-be-sorted" signal is given by the control unit, the material is located with help of the detected 'absence of light' of the material against the backlight captured by the visual spectroscopy (VIS) camera and is then blown out (or ejected) by the air nozzle activated at the detected location. The sensor setup is shown in Figure 2 below.

The experiments were performed by selecting the following pre-processing settings on the Sqalar software – spatial correction, intensity calibration, bad pixel replacement, noise suppression, 1st derivative, smoothing, and normalization. A threshold setting of 105 was selected for all three experimental analyses. Threshold instructs the software on which bandwidth of the spectra should be considered to detect the material. A maximum threshold will result in the machine erroneously detecting a sample as the wrong material. On the other hand, a minimum threshold will make it difficult for the machine to detect anything.

There are two main steps of working with the sorter, namely creating the recipe, where the sorter is taught the NIR spectra of a particular material and then testing the created recipe, i.e. the sample of the taught material is then detected and ejected. For each of the samples, 6 points on

Legend
1. Chute
2. Conveyer belt
3. Sample material
4. NIR light emitter
5. Hyperspectral imaging system & VIS Camera
6. VIS light emitter
7. Control unit
8. Backlight
9. Air nozzle
10. Splitter
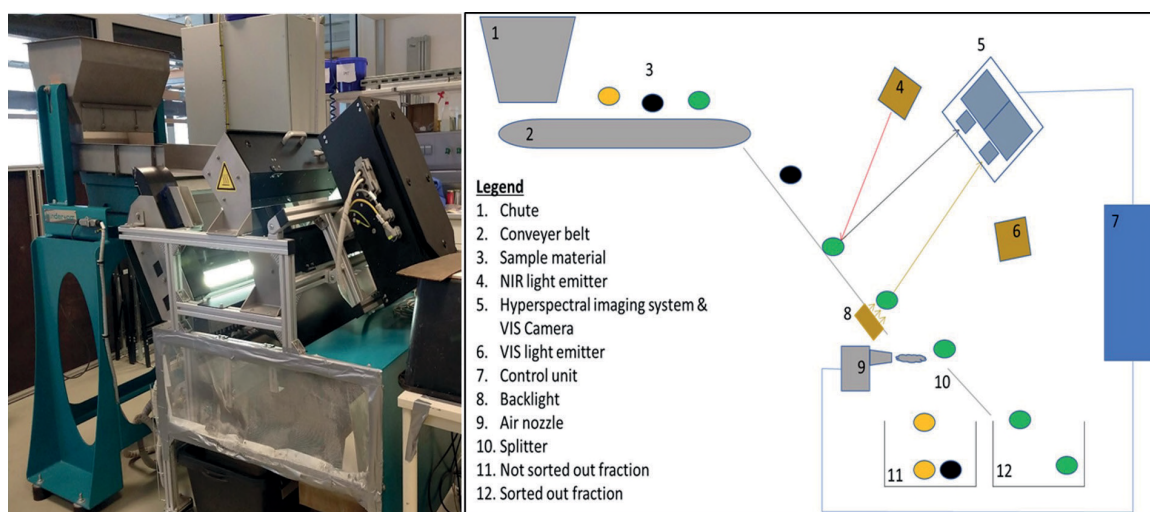11. Not sorted out fraction
12. Sorted out fraction

FIGURE 2: Sensor-based sorting machine at Montanuniversitaet Leoben (Left) and NIR sensor set-up (Right).

the data cube were selected (by avoiding the edge effects) to obtain a mean spectrum, while creating the recipe (a first step above).

2.3 Experiments

Three experiments were conducted to answer the chosen research questions.

- Comparing virgin PLA and conventional plastics spectra: The spectra of 7 conventional plastics and virgin PLA material were analysed using the NIR-based sorter.
- Comparing different grades and thicknesses of virgin PLA samples: The spectra of different grades and thicknesses of virgin PLA material were analysed to identify differences in the spectra due to a change in grade and thickness. Ideally, due to the Beer-Lambert law, the absorption should change in relation to the sample thickness, as the absorption is directly proportional to the sample thickness (Masoumi et al., 2012).
- Testing detection of PLA product samples using virgin PLA recipe: Two sets of experiments were conducted. In the first set, spectra of each of the 10 samples were compared to the virgin PLA spectrum, for which Luminy L175 (1 mm thickness) was used. In the second set, the NIR recipe from Section 2.3.1 with a comparison between conventional plastic and the L175 (1 mm) PLA was used to test whether the 10 PLA product samples are detected & ejected as PLA. Here two different subsets of experiments were conducted, with 10 trials for each-
  - Sequence – here, the 10 samples were scanned in sequence as in Table 1.
  - Product repetition – here, each of the 10 samples was scanned 10 times, before moving to the next product.

The reason for doing this was to check whether the method of scanning the samples would affect the detection results in any way. For both the experiments, conventional plastics were also passed through the sorter to check whether any of them were falsely detected as PLA.

3. RESULTS AND DISCUSSION

3.1 Comparison between conventional plastic and PLA

Figure 3 (a) shows the smoothened and normalized first derivatives of the spectra of the 7 conventional plastics and PLA. As can be seen, PLA has a distinct spectrum from the other 7 conventional plastics. The diagnostic features for PLA are observed in the three selected ranges:

- Range 1 (nm) – 1123 to 1205.
- Range 2 (nm) – 1339 to 1402.
- Range 3 (nm) – 1602 to 1677.

Figure 3 (b) also shows the spectra with only PLA in view and other spectra in grey, to better understand the variation of the PLA spectrum with respect to that of the 7 conventional plastics. As seen PLA has a different spectrum than the 7 conventional plastics.

3.2 Comparison between different grades and thickness of PLA

For this comparison, the normalization setting in the Sqalar software was turned off to compare the two spectra visually. With the normalization setting, the Sqalar software normalizes each spectrum with its maximum peak; thus, the resulting pre-processed spectrum does not represent the correct change in intensities.

Figure 3 (c) shows the processed spectra of PLA of two different grades and thicknesses. It can be observed that the intensities of the recognizable peaks increase with increasing thickness, but the wavelengths where these peaks occur remain constant. This result is in line with the Beer-Lambert law of spectroscopy, which states that the absorption is directly proportional to the thickness of the samples (Masoumi et al., 2012). It is also interesting to note that both the PLA grades of 1 mm have mostly similar intensities; however, the ones with 2 mm are significantly different. However, this does not affect the detection and ejection of PLA of different thicknesses. The following three ranges were selected for the analysis:

- Range 1 (nm) – 1092 to 1167.
- Range 2 (nm) – 1311 to 1517.
- Range 3 (nm) – 1586 to 1677.

Additionally, a principal component analysis was conducted using MATLAB and it showed that the comparisons were separable. Figure 4 (a) shows a PCA loading plot and 3D PCA scatter plot for comparison between two different grades (L175 and 4043) and Figure 4 (b) for two different thicknesses of the same grade (4043 1mm and 2mm). The results showed that the comparisons are separable with almost 100% of variance as illustrated by the first principal component. However, it is important to note that this PCA is only limited to highlighting the difference using the first component and does not reflect on the sorting of the materials.

3.3 Testing the created recipe with PLA product samples

3.3.1 Comparing virgin PLA spectrum with PLA product sample spectrum

The spectra of the 10 PLA products were observed for three ranges of wavelengths and for 10 selected regions with preprocessing settings of 1st derivative, smoothing, and normalization.

- Range 1 (nm) – 1114 to 1267.
- Range 2 (nm) – 1370 to 1414.
- Range 3 (nm) – 1502 to 1543.

Since all 4 virgin PLA samples have the same recognizable peaks with varying intensities, Luminy L175 (1 mm) was selected as the virgin PLA sample to teach the sorter. The selected three ranges and the 10 regions on the spectra (A to J) are shown in Figure 5 on the spectrum of Luminy L175 (1 mm). Each product's spectrum was observed for the selected 3 ranges and 10 regions, and it was seen
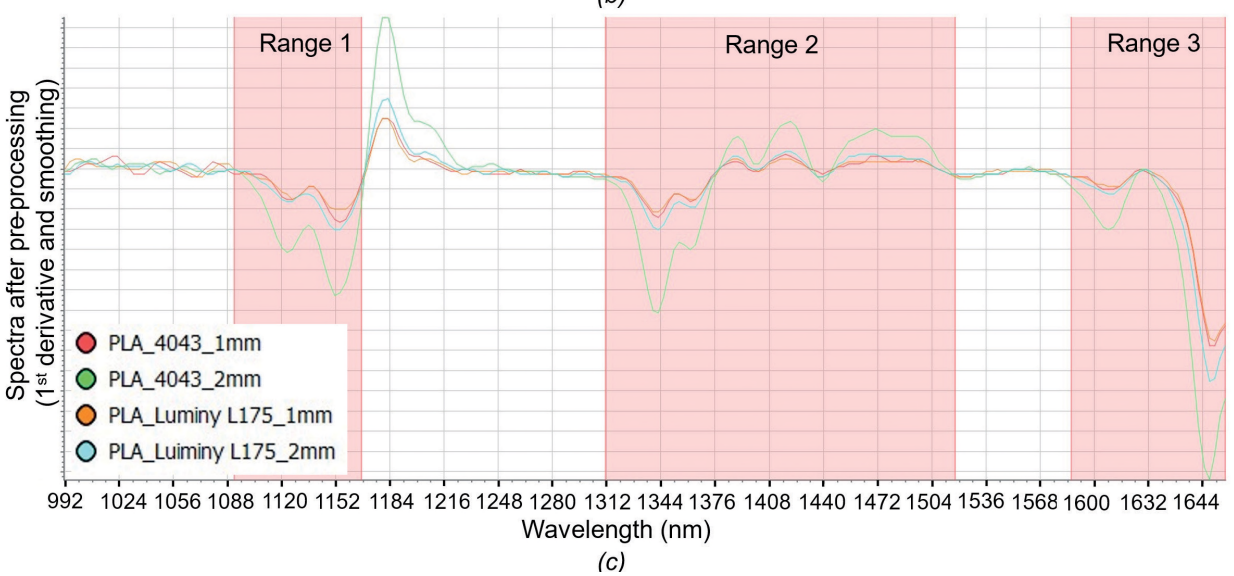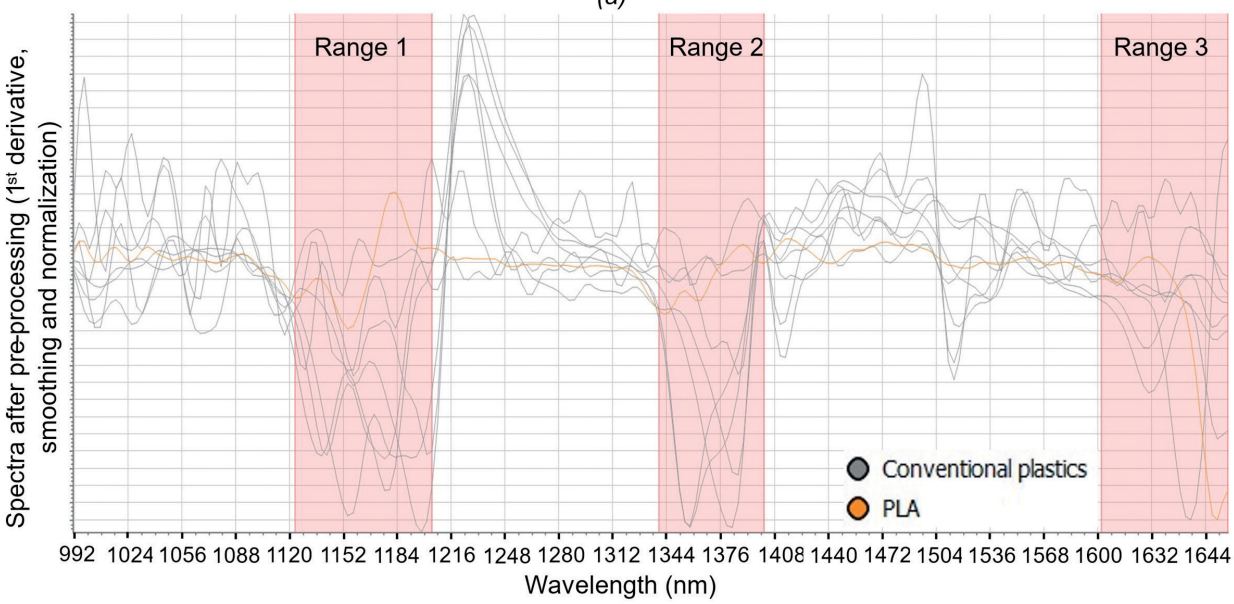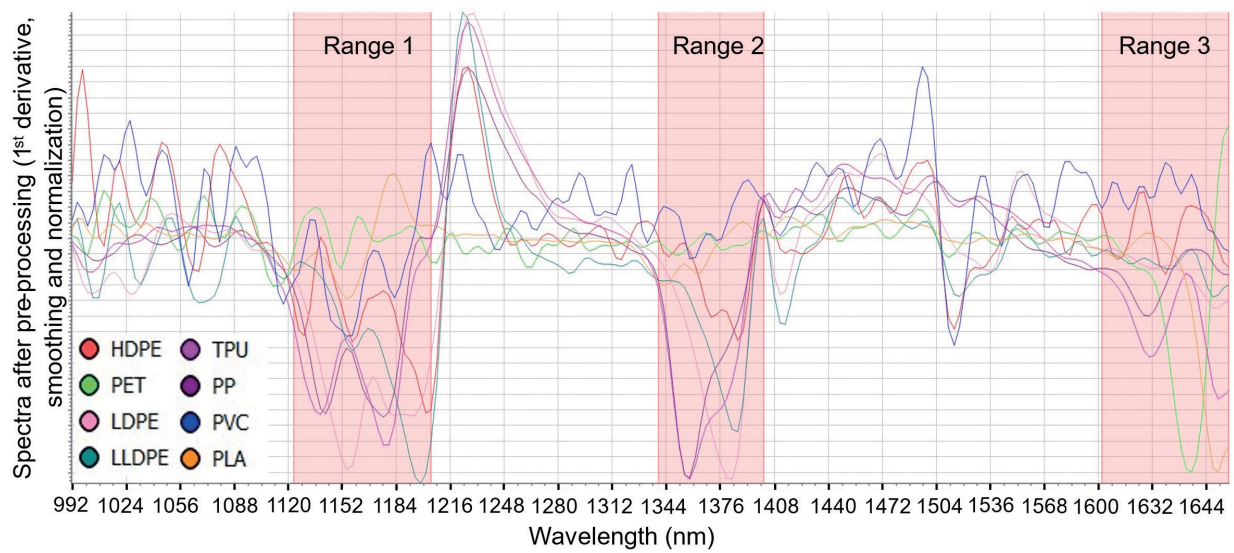
FIGURE 3: (a) Comparison between PLA and conventional plastic spectra; (b) Distinguishing PLA from conventional plastic spectra; (c) Comparison between spectra of different grades and thicknesses of PLA.
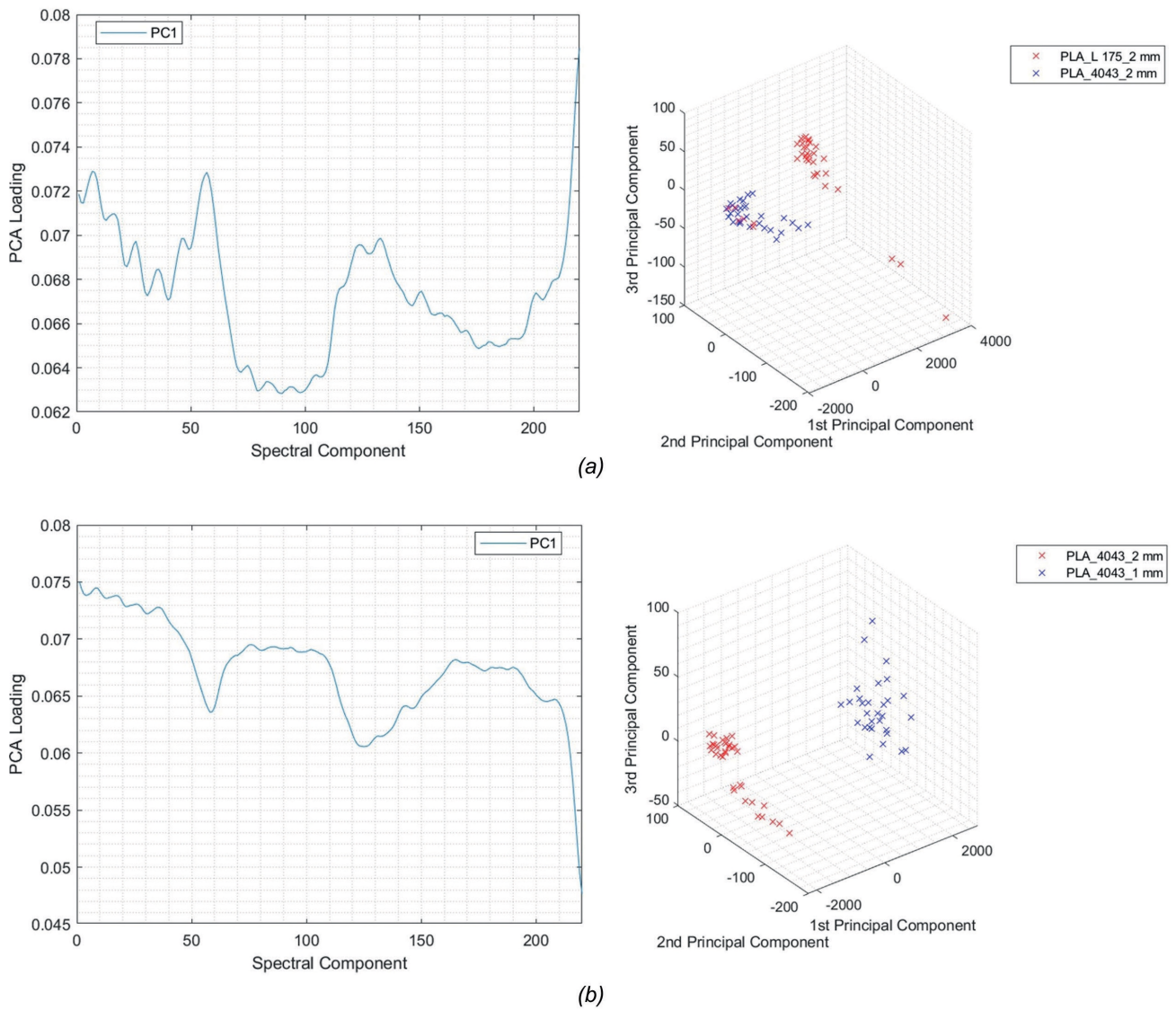
FIGURE 4: (a) Comparing different grades of PLA: PCA loading plot, PC1 – first principal component (Left) and PCA 3D scatter plot (Right); (b) Comparing different thicknesses of PLA: PCA loading plot, PC1 - first principal component (Left) and PCA 3D scatter plot (Right).
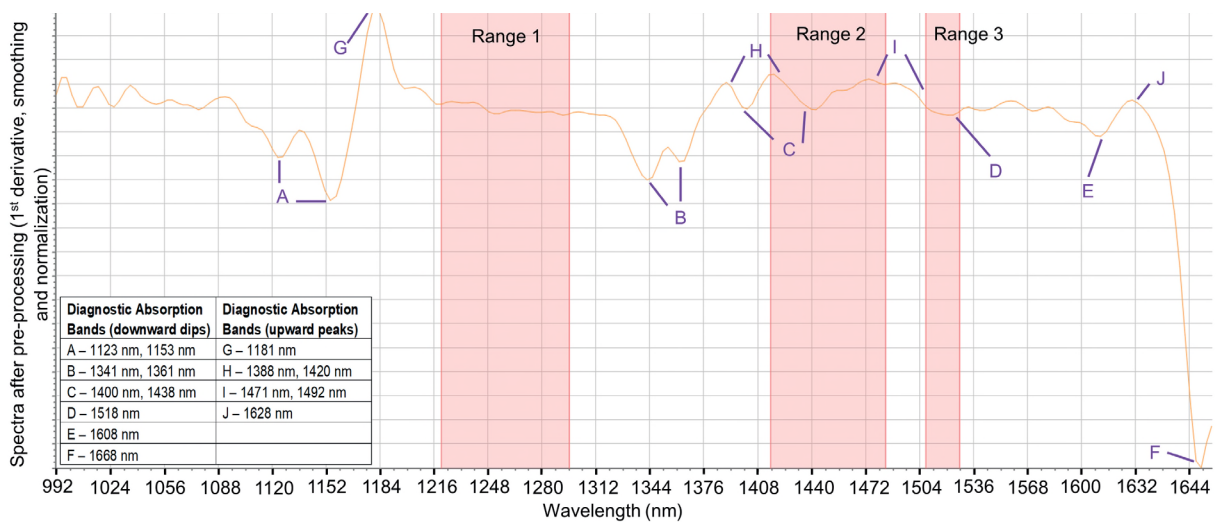

Diagnostic Absorption Bands (downward dips)	Diagnostic Absorption Bands (upward peaks)
A – 1123 nm, 1153 nm	G – 1181 nm
B – 1341 nm, 1361 nm	H – 1388 nm, 1420 nm
C – 1400 nm, 1438 nm	I – 1471 nm, 1492 nm
D – 1518 nm	J – 1628 nm
E – 1608 nm	
F – 1668 nm	

FIGURE 5: Virgin PLA Luminy L175 (1 mm) spectrum with 10 selected regions with the corresponding wavelengths (in the box) selected for analyses along with the three selected ranges.
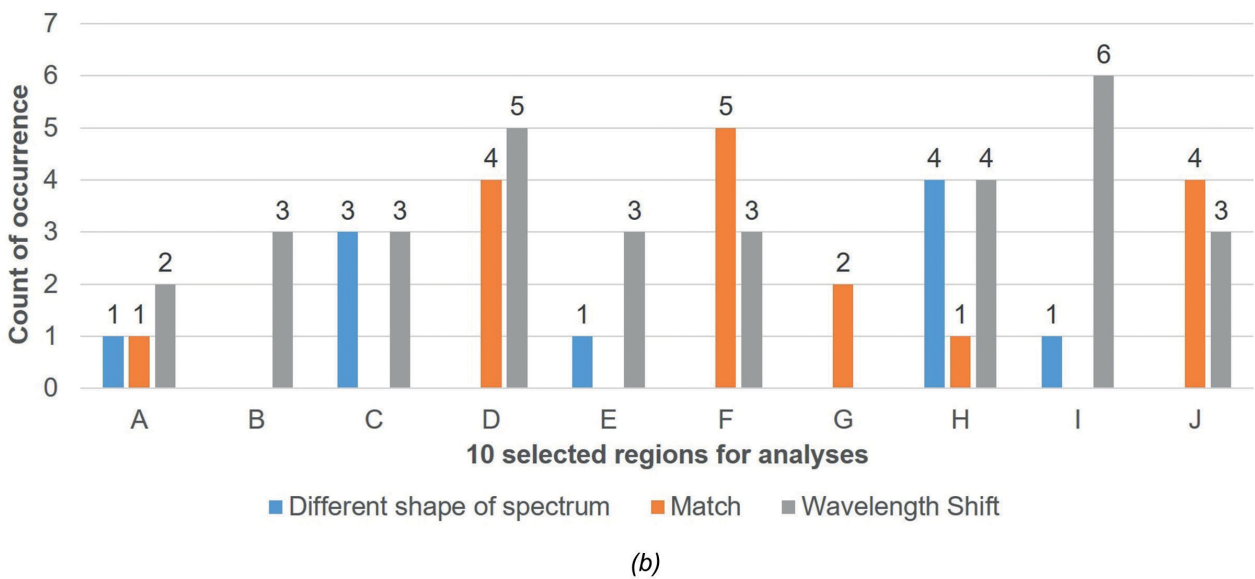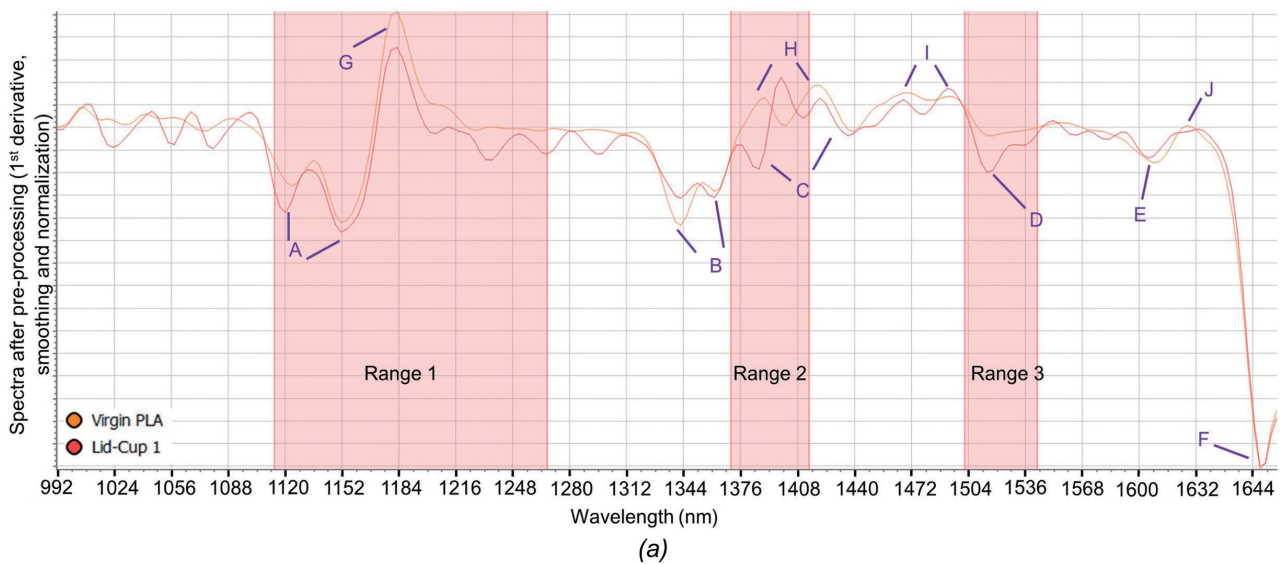
(a)

(b)

FIGURE 6: (a) Comparison between virgin PLA and Lid-Cup 1 product spectra; (b) Comparison between PLA sample product and virgin PLA spectra.
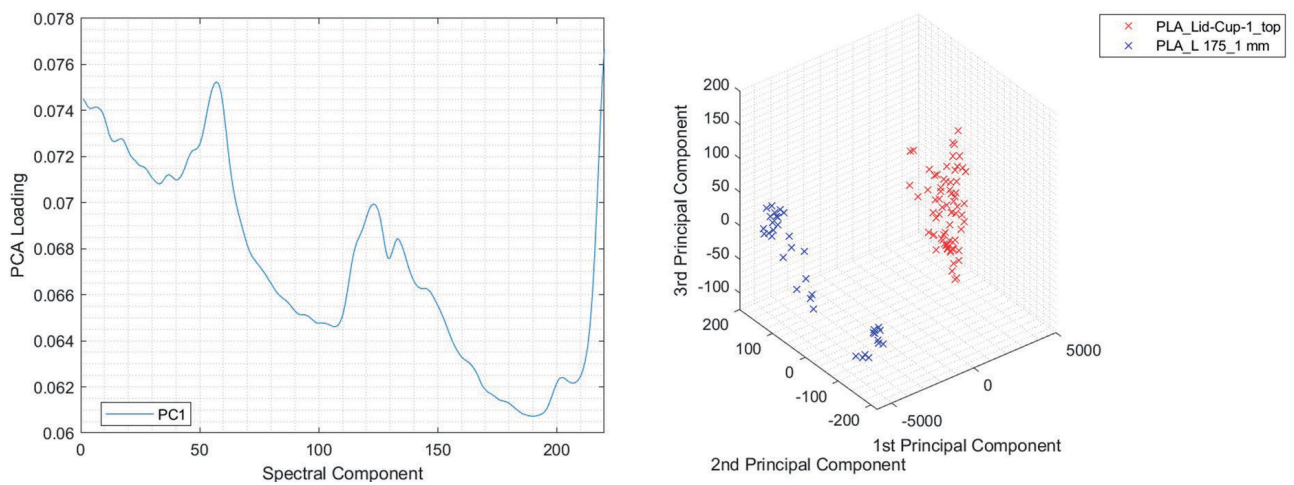

FIGURE 7: Comparing virgin PLA L175_1 mm and Lid-Cup 1: PCA loading plot, PC1 - first principal component (Left) and PCA 3D scatter plot (Right).
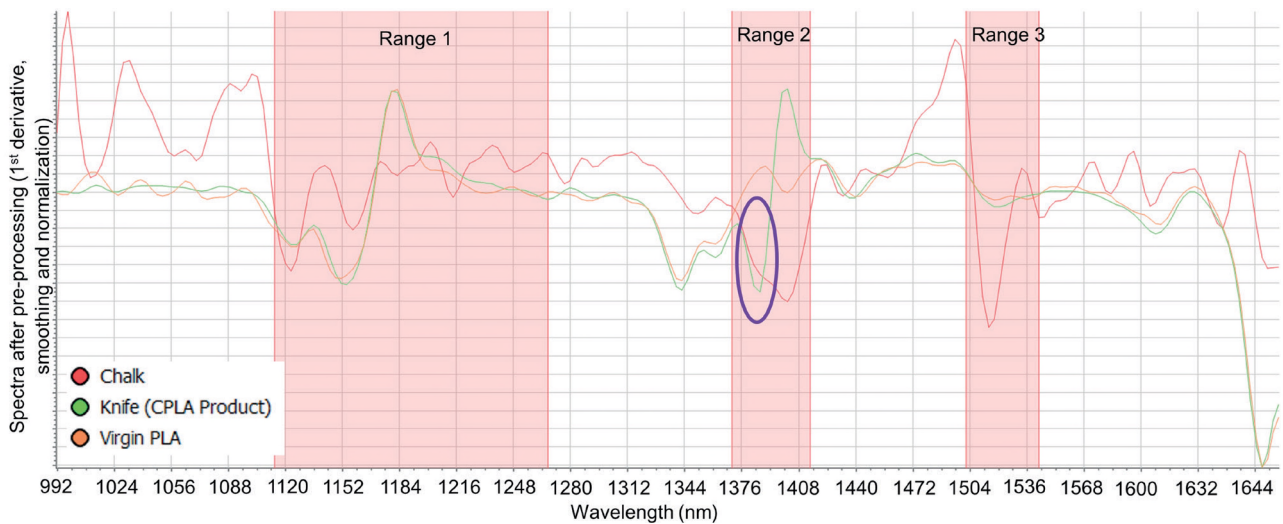
FIGURE 8: Comparison between Chalk, Knife (CPLA Product), and virgin PLA spectra.

that the spectrum either produced a shift of the wavelength at which the diagnostic peak was present or had a different shape of a spectrum than the virgin PLA.

For example, Figure 6 (a) shows a comparison between the spectrum of virgin PLA L175 (1 mm) and the Lid-Cup 1 PLA product sample. It can be seen that there is a wavelength shift in the region A, D & I, one match at F, and different shapes of the spectrum at C & H. It was assumed that the difference in the spectra between the virgin PLA and the PLA product was due to the presence of certain fillers and additives.

A visual comparison between the spectra of every product with virgin PLA for the 10 selected regions (Figure 5) was conducted and it was observed that the most common variation was with respect to a wavelength shift, which is illustrated in Figure 6 (b). It was noticed that the CPLA material samples (Lid-Cup 1, Cutlery 1_Knife, Cutlery 2_Spoon) resulted in different shapes of the spectrum at points C and H - Figure 6(a). The principal component analysis (PCA), conducted with the virgin PLA and PLA products, showed that the comparisons were separable. Figure 7 shows a PCA loading plot and 3D PCA scatter plot for comparison between virgin PLA L175_1 mm and Lid-Cup 1. The results showed that the comparisons are separable with almost 100% of variance as illustrated by the first principal component. However, it is important to note that this PCA is only limited to highlighting the difference using the first component and does not reflect on the sorting of the materials.

Additionally, the variation in spectra of the 10 samples was also observed for the 3 selected ranges. It was observed that range 2 mostly had a different shape of the spectrum than that of the virgin PLA. One of the possible reasons was due to the presence of chalk in the CPLA material (biofutura, 2021) for 3 of the 10 samples (Lid-Cup 1, Cutlery 1_Knife, and Cutlery 2_Spoon).

A chalk sample, obtained from a classroom, was used to see if there was any similarity between the spectrum of chalk and the product. From Figure 8 comparing the spectra of chalk, knife (CPLA material), and PLA Luminy L175 (1

mm), it can be seen that the chalk spectrum differs from the other two materials, except at 1384 nm wavelength. In wavelength range 2, where the CPLA spectrum differs from the virgin PLA spectra, there is a similar recognizable peak in the chalk and CPLA spectra (at 1384 nm - violet mark in Figure 8). Thus, it can be concluded that the different peak is due to the presence of chalk ($CaCO_3$).

3.3.2 Testing sortability of PLA product samples using virgin PLA recipe

The NIR recipe of section 3.1 (Conventional plastics and PLA) was used to check if the PLA products could be detected & blown out with the air nozzle, based on a virgin PLA recipe. Thus, even if the PLA products were having slightly different spectra than the virgin PLA (section 3.3.1), for the selected three ranges the PLA products were successfully detected as PLA. However, it was also found that the ejection of the products was influenced by the backlight settings.

It was observed that not all the PLA products were sorted out as PLA. For example, 3 PLA products (Cup 1, Cup 2, and Container 2) out of the 10, were not sorted out for all 20

		ACTUAL	
		PLA	**CONVENTIONAL PLASTICS**
PREDICTED	**PLA**	*True Positive* 155	*False Positive* 0
	CONVENTIONAL PLASTICS	*False Negative* 45	*True Negative* 140

FIGURE 9: Confusion matrix depicting results of the 20 sorting trials.

Indicator	Formula	Calculated Value
Recall	TP/(TP+FN)	155/(155+45) = 77.5%
Accuracy	(TP+TN)/(TP+TN+FP+FN)	(155+140)/(155+140+0+45) = 86.76%
Precision	TP/(TP+FP)	155/(155+0) = 100%
Sensitivity	TP/(TP+FN)	155/(155+45) = 77.5%
Specificity	TN/(TN+FP)	140/(140+0) = 100%

trials (for both Experiments I and II). A confusion matrix was prepared to present the results of the sorting experiments, where the two classes considered were PLA and conventional plastics (Figure 9). The confusion matrix was created based on the observed performance of the 10 PLA products & 7 conventional plastics – whether they were ejected or not using the virgin PLA recipe. The confusion matrix was manually formulated, without using machine learning. Considering the total 340 units (200 units for 20 trials of 10 PLA products (Section 2.3) and 140 units for 20 trials for 7 conventional plastics), for a sorter setting to sort out virgin PLA, the following results were obtained: 155 True Positives (when PLA was sorted out), 45 False Negatives (when PLA was not sorted out), 140 True Negatives (when conventional plastics were not sorted out as PLA) and 0 False Positives (when conventional plastics were sorted out as PLA).

Using these values the relevant evaluation measures were calculated and are presented below in Table 2 (Kotu & Deshpande, 2018; Saito & Rehmsmeier, 2015).

After observing the output in Sqalar software, it was found that the above results were obtained with a backlight intensity of 20%. And that all 10 products were detected as PLA for all 20 trials (for both Experiment I and II); however, 3 PLA products (Cup 1, Cup 2, and Container 2) out of the 10, were not blown out by the air nozzle. Figure 10 (a) shows the products which were blown out in one of the trials along with their respective false colour images in Sqalar software – orange colour denoting virgin PLA (see Figure 8). In Experiment I (Sequence), Cup 1 was blown out 5 out of 10 times, Cup 2 was ejected 2 out of 10 times and Container 2 was not ejected at all. On the other hand, in Experiment
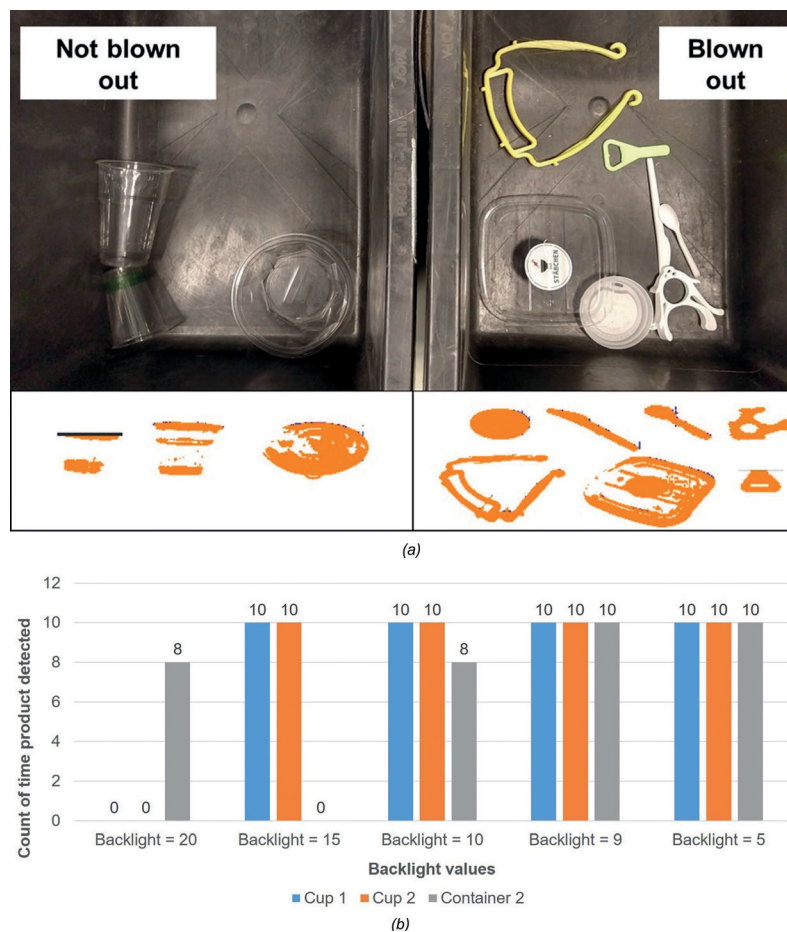

(a)

(b)

FIGURE 10: (a) Products blown out with the virgin PLA recipe (Top-right) and products which were not blown out (Top-left) at 20% backlight intensity, with their respective false colour images (Below); (b) Effect of backlight intensity on transparent PLA product ejection.

II (Product repetition), Cup 1 was blown out for 8 out of 10 trials, whereas Cup 2 and Container 2 were not blown out.

After obtaining the results, another experiment was conducted to see if reducing the backlight intensity influences the ejection of the 3 PLA products (Cup 1, Cup 2, and Container 2). It was observed that the ejection of these 3 PLA products was gradually improved as the backlight intensity was reduced. Experiment I was repeated with the 3 PLA products at intervals of 5 of backlight intensity from 20 to 5%. It was observed that at 5% backlight intensity all the 3 products were blown out all 10 times. Additionally, it was found that 9% is the maximum backlight intensity at which all the 3 products were correctly blown out as PLA all 10 times. These results are illustrated in Figure 10 (b). The reason for this behavior is that since the three materials are transparent, all the backlight is transmitted through these products; thus, producing no 'absence of light' and making it difficult to identify the location of the detected product (section 2.2). So, it could be said that even though the product was detected as PLA - Figure 10 (a), it could not be shot out because of the inability of the system to identify its location, causing the non-functioning of the air nozzle. As a result, the ejection improved once the backlight intensity was reduced - Figure 10 (b). This led to the recall, accuracy, and sensitivity of 100%.

4. CONCLUSIONS

Sorting experiments conducted using the lab-scale chute type NIR sorting system in MUL with virgin polymer materials showed that PLA has a distinct spectrum than HDPE, PET, LDPE, LLDPE, TPU, PP, and PVC - Figure 3 (a) and (b); and thus, could be ideally sorted out from a mixed plastic fraction.

The change in grade and thickness of virgin PLA resulted in varying intensities of the spectra. However, there was no observed shift in the wavelengths of the diagnostic peaks. This result was in line with the Beer-Lambert law which states that the absorption is directly proportional to the sample thickness.

It was also seen that the spectra of the PLA products varied from that of the virgin PLA mostly with a shift in wavelength and a difference in the shape of spectra, due to some fillers like calcium carbonate. But this effect doesn't affect the detection and the ejection of these products by the NIR sensor-based sorting equipment. Also, with proper backlight intensity setting all 10 PLA product samples were detected & blown out using the NIR recipe created from the virgin PLA material; thus, improving the values of recall, accuracy, and sensitivity of the confusion matrix. The backlight intensity particularly affected the transparent PLA products (Cup 1, Cup 2, and Container 2), whereas the other products were easily detected & ejected with the highest selected backlight setting of 20%. Thus, it was observed that an appropriate backlight setting (in the used chute-type sorter) is important to be able to correctly sort the transparent PLA products.

ACKNOWLEDGEMENTS

REFERENCES

Alaerts, L., Augustinus, M., & van Acker, K. (2018). Impact of Bio-Based Plastics on Current Recycling of Plastics. Sustainability, 10(5), 1487. https://doi.org/10.3390/su10051487

Amigo, J. M., Babamoradi, H., & Elcoroaristizabal, S. (2015). Hyperspectral image analysis. A tutorial. Analytica Chimica Acta, 896, 34–51. https://doi.org/10.1016/j.aca.2015.09.030

biofutura. (2021, May 27). CPLA Material | Bio Futura - Sustainable. https://www.biofutura.com/en/materials/cpla

Bonifazi, G [Giuseppe], Gasbarrone, R., & Serranti, S [Silvia] (2021). Detecting CONTAMINANTS IN POST-CONSUMER PLASTIC PACKAGING WASTE BY A NIR HYPERSPECTRAL IMAGING-BASED CASCADE DETECTION APPROACH. Detritus, Volume 15- June 2021. https://doi.org/10.31025/2611-4135/2021.14086

Briassoulis, D., Pikasi, A., & Hiskakis, M. (2020). Recirculation potential of post-consumer /industrial bio-based plastics through mechanical recycling - Techno-economic sustainability criteria and indicators. Polymer Degradation and Stability, 109217. https://doi.org/10.1016/j.polymdegradstab.2020.109217

Calabrò, P. S., & Grosso, M. (2018). Bioplastics and waste management. Waste Management (New York, N.Y.), 78, 800–801. https://doi.org/10.1016/j.wasman.2018.06.054

Cao, J., & Sharma, S. (2013). Near-Infrared Spectroscopy for Anticounterfeiting Innovative Fibers. ISRN Textiles, 2013, 1–4. https://doi.org/10.1155/2013/649407

Chen, X., Kroell, N., Li, K., Feil, A., & Pretz, T. (2021). Influences of bioplastic polylactic acid on near-infrared-based sorting of conventional plastic. Waste Management & Research : The Journal of the International Solid Wastes and Public Cleansing Association, ISWA, 734242X211003969. https://doi.org/10.1177/0734242X211003969

DIRECTIVE 2008/98/EC OF THE EUROPEAN PARLIAMENT AND OF THE COUNCIL of 19 November 2008 on waste and repealing certain Directives 1 (2008). https://eur-lex.europa.eu/legal-content/EN/TXT/PDF/?uri=CELEX:02008L0098-20180705&from=EN

Friedrich, K [Karl], Koinig, G [Gerald], Fritz, T., Pomberger, R., & Vollprecht, D [Daniel] (2022). Sensor-based and Robot Sorting Processes and their Role in Achieving European Recycling Goals - A Review. Academic Journal of Polymer Science, 5(4), 1–18. https://doi.org/10.19080/AJOP.2021.05.555668

Friedrich, K [Karl], Koinig, G [Gerald], Pomberger, R., & Vollprecht, D [Daniel] (2022). Qualitative analysis of post-consumer and post-industrial waste via near-infrared, visual and induction identification with experimental sensor-based sorting setup. MethodsX, 9, 101686. https://doi.org/10.1016/j.mex.2022.101686

Gere, D., & Czigany, T. (2019). Recycling of Mixed Poly(Ethylene-terephthalate) and Poly(Lactic Acid). MATEC Web of Conferences, 253, 2005. https://doi.org/10.1051/matecconf/201925302005

Ghasemzadeh-Barvarz, M., Rodrigue, D., & Duchesne, C. (2014). Multivariate image analysis for inspection of multilayer films. Polymer Testing, 40, 196–206. https://doi.org/10.1016/j.polymertesting.2014.09.011

Hahladakis, J. N., & Iacovidou, E. (2018). Closing the loop on plastic packaging materials: What is quality and how does it affect their circularity? The Science of the Total Environment, 630, 1394–1400. https://doi.org/10.1016/j.scitotenv.2018.02.330

Hahladakis, J. N., & Iacovidou, E. (2019). An overview of the challenges and trade-offs in closing the loop of post-consumer plastic waste (PCPW): Focus on recycling. Journal of Hazardous Materials, 380, 120887. https://doi.org/10.1016/j.jhazmat.2019.120887

Helena Wedin, C. Gupta, Pailak Mzikian, F. Englund, R. Hornbuckle, Vittoria Troppenz, Lucijan Kobal, M. Costi, D. Ellams, & S. Olsson (2017). Title : Can automated NIR technology be a way to improve the sorting quality of textile waste ? In

Koinig, G [G.], Friedrich, K [K.], Rutrecht, B [B.], Oreski, G., Barretta, C [C.], & Vollprecht, D [D.] (2022). Influence of reflective materials, emitter intensity and foil thickness on the variability of near-infrared spectra of 2D plastic packaging materials. Waste Management (New York, N.Y.), 144, 543–551. https://doi.org/10.1016/j.wasman.2021.12.019

Koinig, G [Gerald], Rutrecht, B [Bettina], Friedrich, K [Karl], Barretta, C [Chiara], & Vollprecht, D [Daniel] (2022). Latent Recycling Potential of Multilayer Films in Austrian Waste Management. Polymers, 14(8), 1553. https://doi.org/10.3390/polym14081553

Kotu, V., & Deshpande, B [Bala]. (2018). Chapter 8 - Model Evaluation. In V. Kotu & B. Deshpande (Eds.), Data science: Concepts and practice / Vijay Kotu, Bala Deshpande (pp. 263–279). Morgan Kaufmann. https://doi.org/10.1016/B978-0-12-814761-0.00008-3

Lorber, K., Kreindl, G., Erdin, E., & Sarptaş, H. (2015). Waste Management Options for Biobased Polymeric Composites. In

Manley, M. (2014). Near-infrared spectroscopy and hyperspectral imaging: Non-destructive analysis of biological materials. Chemical Society Reviews, 43(24), 8200–8214. https://doi.org/10.1039/C4CS00062E

Masoumi, H., Safavi, S. M., & Khani, Z. (2012). Identification and classification of plastic resins using near infrared reflectance spectroscopy. International Journal of Mechanical and Industrial Engineering, 6, 213–220.

Müller, G., Hanecker, E., Blasius, K., Seidemann, C., Tempel, L., Sadocco, P., Pozo, B. F., Boulougouris, G., Lozo, B., Jamnicki, S., & Bobu, E. (2014). End-of-life Solutions for Fibre and Bio-based Packaging Materials in Europe. Packaging Technology and Science, 27(1), 1–15. https://doi.org/10.1002/pts.2006

Neo, E. R. K., Yeo, Z., Low, J. S. C., Goodship, V., & Debattista, K. (2022). A review on chemometric techniques with infrared, Raman and laser-induced breakdown spectroscopy for sorting plastic waste in the recycling industry. Resources, Conservation and Recycling, 180, 106217. https://doi.org/10.1016/j.resconrec.2022.106217

Niaounakis, M. (2019). Recycling of biopolymers – The patent perspective. European Polymer Journal, 114, 464–475. https://doi.org/10.1016/j.eurpolymj.2019.02.027

Pieszczek, L., & Daszykowski, M. (2019). Improvement of recyclable plastic waste detection – A novel strategy for the construction of rigorous classifiers based on the hyperspectral images. Chemometrics and Intelligent Laboratory Systems, 187, 28–40. https://doi.org/10.1016/j.chemolab.2019.02.009

Rani, M., Marchesi, C., Federici, S., Rovelli, G., Alessandri, I., Vassalini, I., Ducoli, S., Borgese, L., Zacco, A., Bilo, F., Bontempi, E., & Depero, L. E. (2019). Miniaturized Near-Infrared (MicroNIR) Spectrometer in Plastic Waste Sorting. Materials (Basel, Switzerland), 12(17). https://doi.org/10.3390/ma12172740

Rodarmel, C., & Shan, J. (2002). Principal Component Analysis for Hyperspectral Image Classification. Surveying and Land Information Systems, 62(2), 115-000. https://engineering.purdue.edu/~jshan/publications/2002/SaLIS_2002_HyperImagesPCA.pdf

Saito, T., & Rehmsmeier, M. (2015). The precision-recall plot is more informative than the ROC plot when evaluating binary classifiers on imbalanced datasets. PLOS ONE, 10(3), e0118432. https://doi.org/10.1371/journal.pone.0118432

Serranti, S [Silvia], & Bonifazi, G [Giuseppe]. (2018). 2 - Techniques for separation of plastic wastes. In F. P. Torgal, J. M. Khatib, F. Colangelo, & R. Tuladhar (Eds.), Woodhead Publishing series in civil and structural engineering. Use of recycled plastics in eco-efficient concrete (pp. 9–37). Woodhead Publishing. https://doi.org/10.1016/B978-0-08-102676-2.00002-5

Ulrici, A., Serranti, S [S.], Ferrari, C., Cesare, D., Foca, G., & Bonifazi, G [G.] (2013). Efficient chemometric strategies for PET–PLA discrimination in recycling plants using hyperspectral imaging. Chemometrics and Intelligent Laboratory Systems, 122, 31–39. https://doi.org/10.1016/j.chemolab.2013.01.001

Wu, X., Li, J., Yao, L., & Xu, Z. (2020). Auto-sorting commonly recovered plastics from waste household appliances and electronics using near-infrared spectroscopy. Journal of Cleaner Production, 246, 118732. https://doi.org/10.1016/j.jclepro.2019.118732

Zheng, Y., Bai, J., Xu, J., Li, X., & Zhang, Y. (2018). A discrimination model in waste plastics sorting using NIR hyperspectral imaging system. Waste Management (New York, N.Y.), 72, 87–98. https://doi.org/10.1016/j.wasman.2017.10.015

Zhu, S., Chen, H., Wang, M., Guo, X., Lei, Y., & Jin, G. (2019). Plastic solid waste identification system based on near infrared spectroscopy in combination with support vector machine. Advanced Industrial and Engineering Polymer Research, 2(2), 77–81. https://doi.org/10.1016/j.aiepr.2019.04.001